

## Supporting Information

### **Hexagonal SiC with spatially separated active sites on polar and nonpolar facets achieving enhanced hydrogen production from photocatalytic water reduction**

Da Wang,<sup>ab</sup> Ning Liu,<sup>b</sup> Zhongnan Guo,<sup>a</sup> Wenjun Wang,<sup>b</sup> Liwei Guo,<sup>b</sup> Wenxia Yuan<sup>a\*</sup> and  
Xiaolong Chen<sup>bcd\*</sup>

*a. Department of Chemistry, School of Chemistry and Biological Engineering, University of Science and Technology Beijing, Beijing, 100083, China.*

*b. Research & Development Center for Functional Crystals, Beijing National Laboratory for Condensed Matter Physics, Institute of Physics, Chinese Academy of Sciences, Beijing 100190, China*

*c. Beijing National Laboratory for Condensed Matter Physics, National Laboratory for Superconductivity, Institute of Physics, Chinese Academy of Sciences, Beijing 100190, China*

*d. School of Physical Sciences, University of Chinese Academy of Sciences, Beijing, China.*

*Collaborative Innovation Center of Quantum Matter, Beijing, China*

*E-mail: chenx29@iphy.ac.cn; Fax: +86-010-82649646; [Tel: + 86-010-82649039](tel:+86-010-82649039)*

*E-mail:wxyuanwz@163.com; Fax: +86-010-62333033; [Tel: + 86-010-62332221](tel:+86-010-62332221)*

# 1. Experimental Details

**Table S1** Calculation conditions for geometry optimization and energy task

Task: Geometry optimization		Energy	
Functional	GGA PBE		
Minimizer	Fine quality		
	Energy:	5.0e-6 eV/atom	
	Max force:	0.01 eV/	
	Max stress:	0.02 GPa	
Algorithm	BFGS:	use line search	
Stress	0 for all		
Energy cutoff	310 eV		310 eV
SCF tolerance	5.0*10-7 eV/atom		5.0*10-7 eV/atom
Pseudopotentials	Ultrasoft <sup>3</sup>		Norm-conserving <sup>4</sup>
FFT grid density	Fine quality		Precise
Finite basis correction	Smart		Smart
Electronic minimizer	Density Mixing		Density Mixing
Orbital occupancy	Fixed		Fixed
<i>k</i> point quality	Fine quality		Fine quality
Band structure	Unchecked	Checked	Fine quality k point set
Density of states	Unchecked	Checked	Medium quality k point set

## 1.1 Materials and Reagents

All chemicals are analytical grade and used as received without further purification. Green 6H-SiC powders (99.9% pure, Shanghai ST-nano Science & Technology Co.Ltd.) were first pre-treated in a muffle furnace at 700 °C for 3 h to remove any organic residues, and were immersed in a HF (40%) solution for 24 h to remove the oxides on the surface. Then the powders were washed with deionized water thoroughly and dried at 60°C for 12 h in a vacuum box. The particle size of obtained SiC is about 6 μm. The single crystals of 6H-SiC (Tankeblue Co.Ltd) were cut into wafers with desired facets. These wafers were then grinded and finally chemical and mechanically polished.

## 1.2 Noble metals and/or metal oxides loading by impregnation method.

For comparison, metal loaded catalysts were also prepared by impregnation method. MnO<sub>2</sub> (IM)/SiC was synthesized with Mn(NO<sub>3</sub>)<sub>2</sub> solution as precursor followed by post-calcination at 673 K for 2 h. Similarly, Pt (IM)/ SiC/Co<sub>3</sub>O<sub>4</sub> sample was performed by impregnation of Pt and photo-deposition of Co<sub>3</sub>O<sub>4</sub>, while Pt/SiC/Co<sub>3</sub>O<sub>4</sub> (IM) sample was prepared by photo-deposition of Pt and impregnation of Co<sub>3</sub>O<sub>4</sub>. The samples A (IM)/SiC/B, A/SiC/B (IM) (A=Au, Ag, B=MnO<sub>2</sub>, Co<sub>3</sub>O<sub>4</sub>) were prepared with the similar method.

## 1.3 Computational method and details

Density-function-theory (DFT) calculations in this work were performed using the Cambridge Serial Total Energy Package (CASTEP). Ultrasoft pseudopotential was chosen in the calculations because of its advantages in both efficiency and

credibility. A self-consistent method (tolerance  $5.0 \times 10^{-7}$  eV/atom) was employed with the wave functions expanded in plane waves up to a cutoff energy of 310 eV. Exchange-correlation effects were described by the Perdew-Burke-Ernzerhof (PBE) within generalized gradient approximation (GGA). The first Brillouin zone was sampled with grid spacing of  $0.02 \text{ \AA}^{-1}$ . Geometry optimization was implemented with the Broyden, Fletcher, Goldfarb, and Shannon (BFGS) method until the remnant Hellmann-Feynman forces on the ions were less than  $0.01 \text{ eV \AA}^{-1}$ , and the energy change per atom was less than  $5.0 \times 10^{-6}$  eV (details shown in Table S1).

#### 1.4 Mott-Schottky and photocurrent measurements

SiC photoelectrodes were prepared using Si- $\{0001\}$  and  $\{10-10\}$  facets terminated SiC single crystals, respectively. Mott-Schottky experiments were carried out on a three-electrode electrochemical setup using 0.5 M  $\text{Na}_2\text{SO}_4$  solution as the electrolyte. The SiC photoelectrode, the platinum electrode and the saturated calomel electrode (SCE) were used as the working electrode, the counter electrode and the reference electrode, respectively.

Photocurrent measurements were conducted with the same condition except the catalysts were utilized as working electrodes.

The electrochemical impedance spectroscopy (EIS) measurements were performed in dark and under simulated solar light irradiation by applying voltage with 5 mV amplitude in a frequency range from 0.01 Hz to 100 kHz under open circuit potential conditions in 0.5 M  $\text{Na}_2\text{SO}_4$  solution.

#### 1.5 Photocatalytic activity measurements

The photocatalytic reactions were performed in Labsolar II system (Beijing Perfectlight Technology Co. Ltd.). A 300 mL Pyrex reaction vessel was connected to a closed gas circulation and an evacuation system at ambient temperature. The evolved gases were analyzed by an online gas chromatograph (GC7890II, Techcomp) equipped with a molecular sieve (5 Å pore size) and N<sub>2</sub> carrier gas. Under continuous stirring, 10 mg photocatalysts were dispersed into 100 mL de-ionized water containing 0.1 mol·L<sup>-1</sup> Na<sub>2</sub>S, 0.1 mol·L<sup>-1</sup> Na<sub>2</sub>SO<sub>3</sub> or 0.04 mol·L<sup>-1</sup> AgNO<sub>3</sub> as sacrificial reagents by ultra-sonicating for 5 min. Prior to irradiation, the system was vacuumized for 30 min to remove the dissolved gases in water. A continuous magnetic stirrer was applied at the bottom of the reactor in order to keep the photocatalyst particles in suspension state during the whole experiment. A 300 W Xe lamp was used as a light source and placed 1 cm away from the vessel. A UV cut-off filter ( $\lambda \geq 420\text{nm}$ ) was used to confirm the visible light source for the photocatalytic reactions.

#### 1.6 Photocatalytic activity

The apparent quantum efficiency (AQE) was measured under the same conditions except that the 420 nm cut-off filter was changed to 420 nm band-pass filter. In the experiment, the irradiation intensity after the 420 nm band-pass filter was determined to be 10.1 mW/cm<sup>2</sup>. The reaction solution was irradiated for 4 h to calculate AQE according to the following equation:

$$\text{AQE} = \frac{\text{number of reacted electrons}}{\text{number of incident photons}} \times 100\%$$

$$= \frac{\text{number of evolved H}_2 \text{ molecules} \times 2}{\text{number of incident photons}} \times 100\%$$

## 2. Results

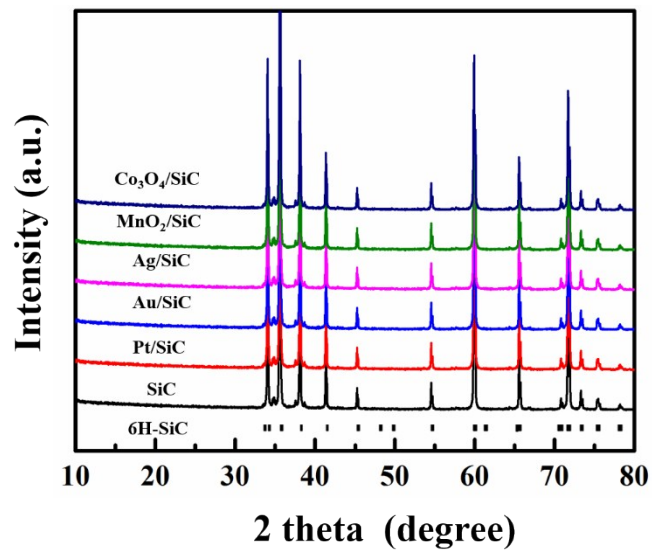


Fig. S1. The XRD patterns of 6H-SiC with photo-deposition of noble metals or metal oxides.

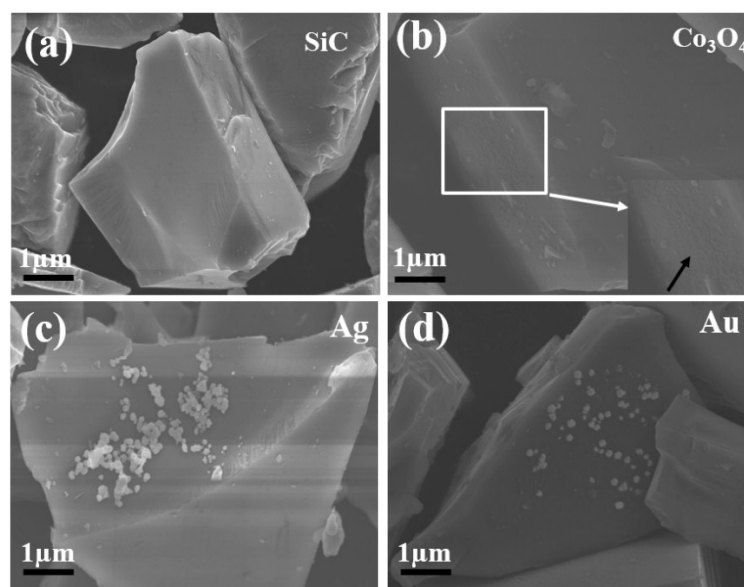


Fig. S2. The SEM images of SiC (a) and SiC with photo-deposition of Co<sub>3</sub>O<sub>4</sub> (b) and

Ag (c) and Au(d).

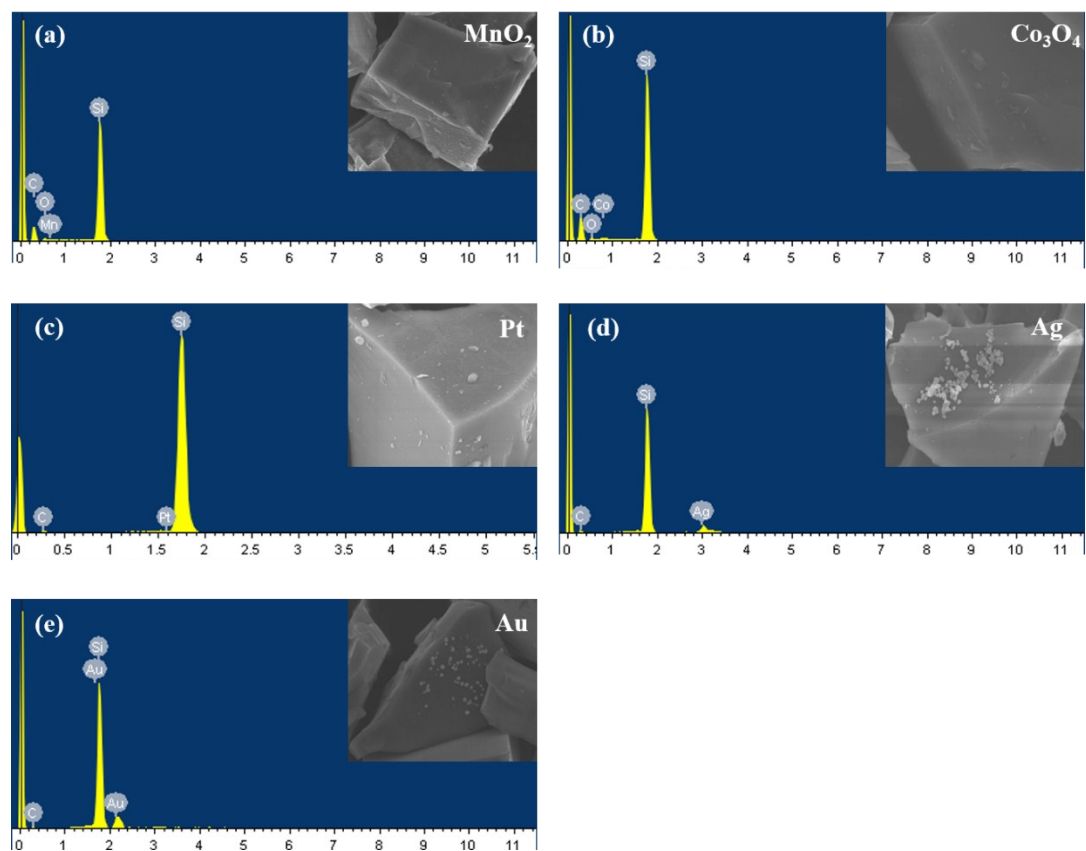


Fig. S3. EDS of Fig. 1 samples: (a) MnO<sub>2</sub>/SiC, (b) Co<sub>3</sub>O<sub>4</sub>/SiC, (c) Pt/SiC, (d) Ag/SiC, (e) Au/SiC.

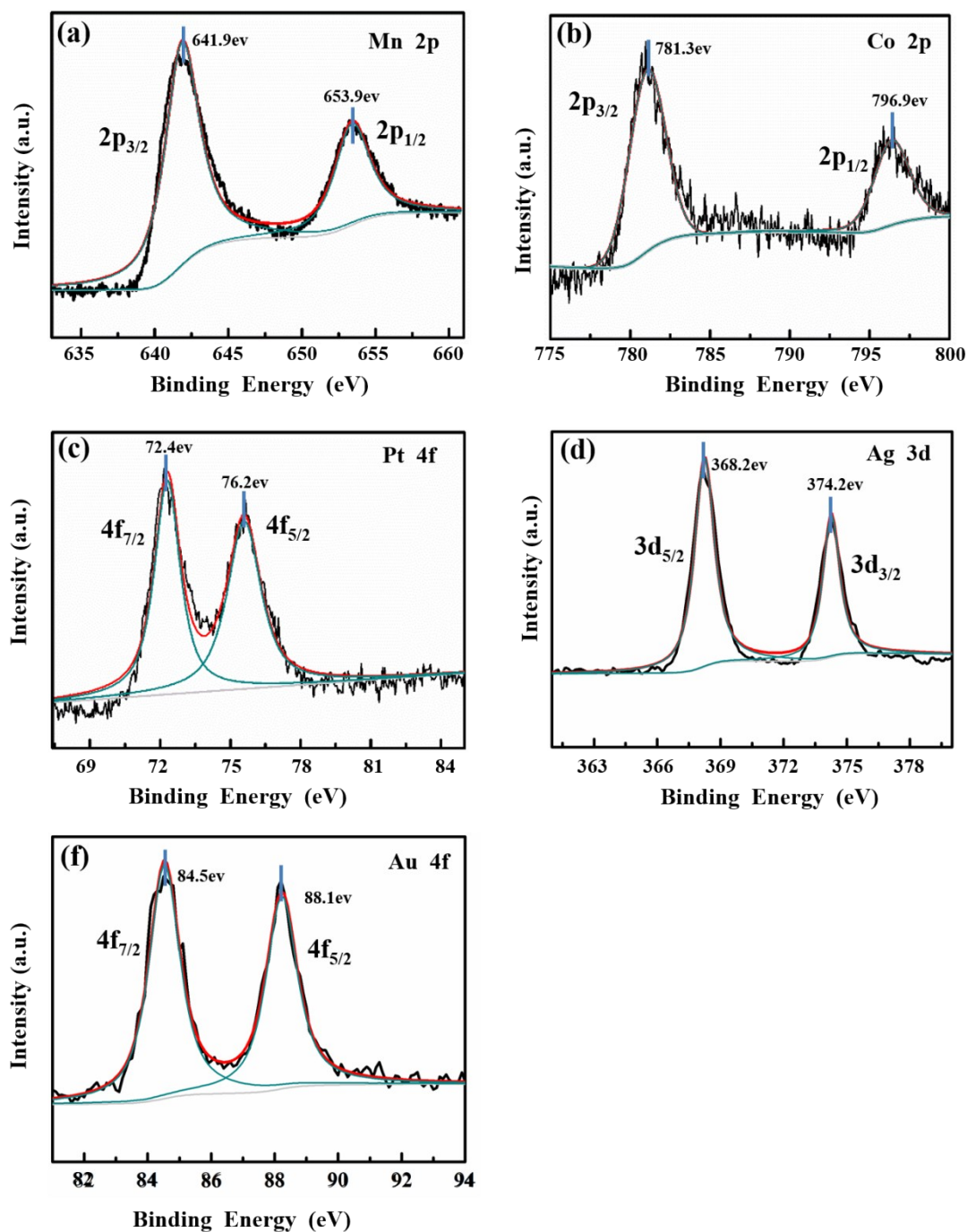


Fig. S4. XPS of typical samples: (a)  $\text{MnO}_2/\text{SiC}$ , (b)  $\text{Co}_3\text{O}_4/\text{SiC}$ , (c)  $\text{Pt}/\text{SiC}$ , (d)  $\text{Ag}/\text{SiC}$ , (e)  $\text{Au}/\text{SiC}$ . The XPS of Pt 4f, Au 4f revealed that the electronic energy of deposited elements were slightly higher than the metallic state (Pt, Au), while the Ag 3d result indicates the element is in the metallic form. According to the binding energy of Co 2p and Mn 2p in XPS, the species can be ascribed to  $\text{Co}_3\text{O}_4$  and  $\text{MnO}_2$ .



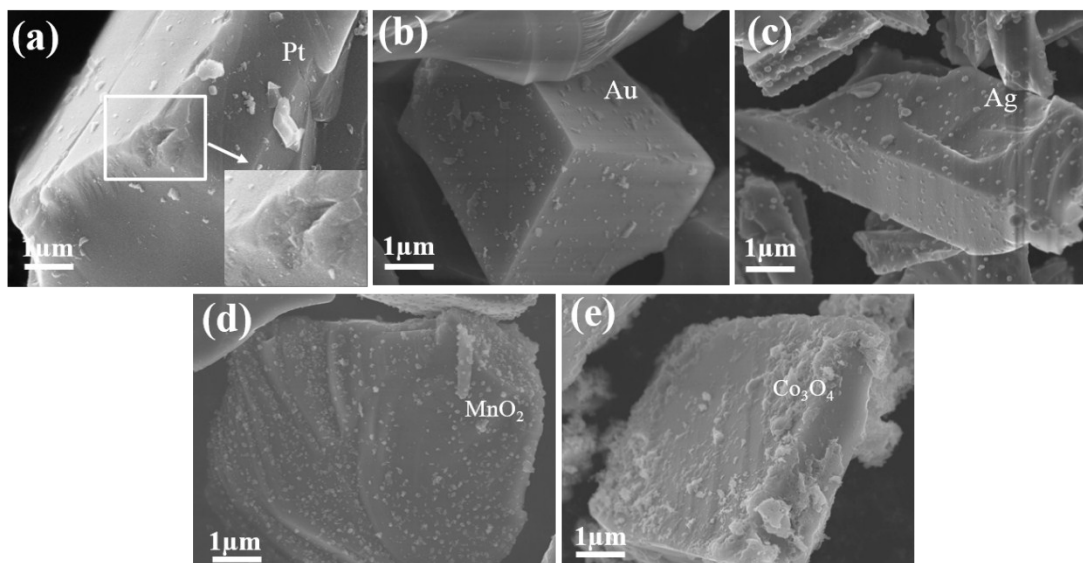


Fig. S5. The SEM images of single cocatalysts deposited on SiC by impregnation method: (a) Pt/SiC, (b) Au/SiC, (c) Ag/SiC, (d) MnO<sub>2</sub>/SiC, (e) Co<sub>3</sub>O<sub>4</sub>/SiC.

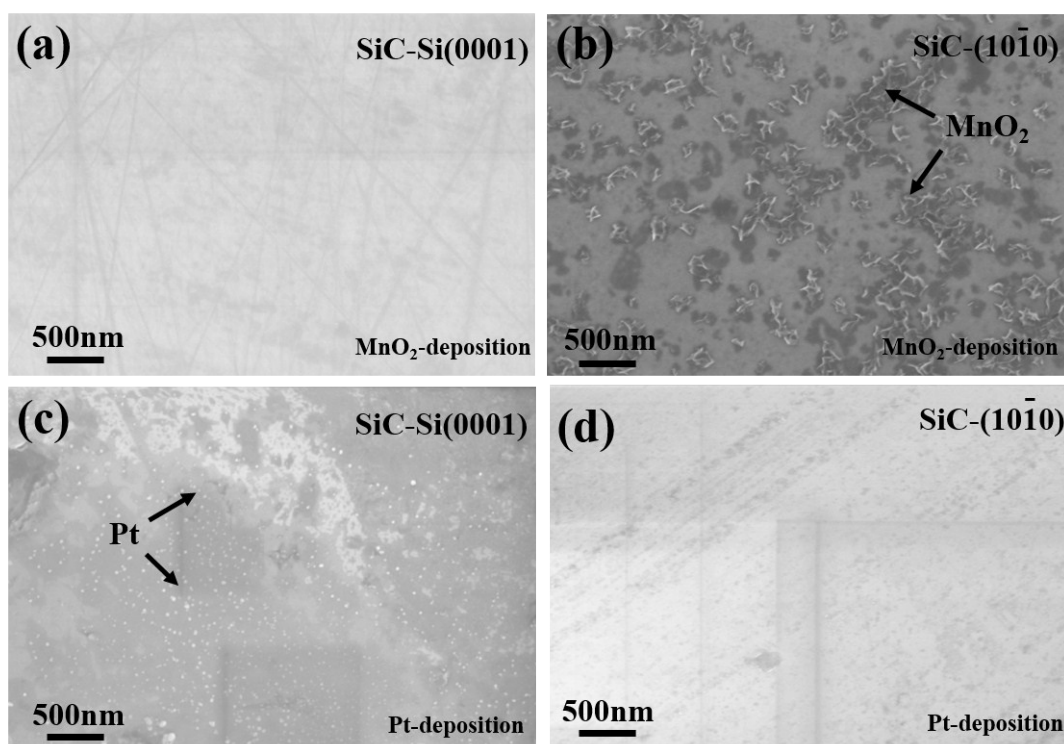


Fig. S6. The SEM images of SiC single crystals with photo-deposition of Pt and MnO<sub>2</sub>, Si- $\{0001\}$  terminated facets for (a) and (c),  $\{10-10\}$  terminated facets for (b) and (d). It can be seen that Pt only deposited on  $\{0001\}$  facets while MnO<sub>2</sub> on  $\{10-10\}$ .

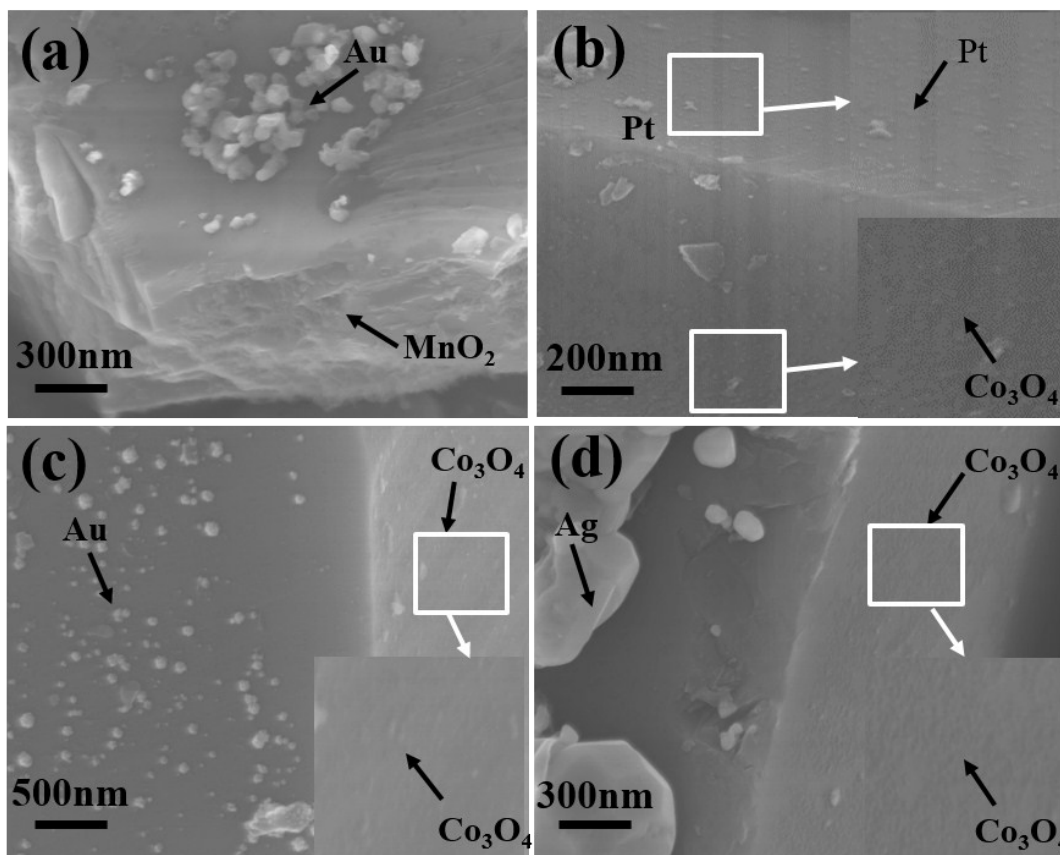


Fig. S7. The SEM images of SiC with photo-deposition of noble metals and metal oxides. (a) Au/SiC/MnO<sub>2</sub>, (b) Pt/SiC/Co<sub>3</sub>O<sub>4</sub>, (c) Au/SiC/Co<sub>3</sub>O<sub>4</sub>, (d) Ag/SiC/Co<sub>3</sub>O<sub>4</sub>.

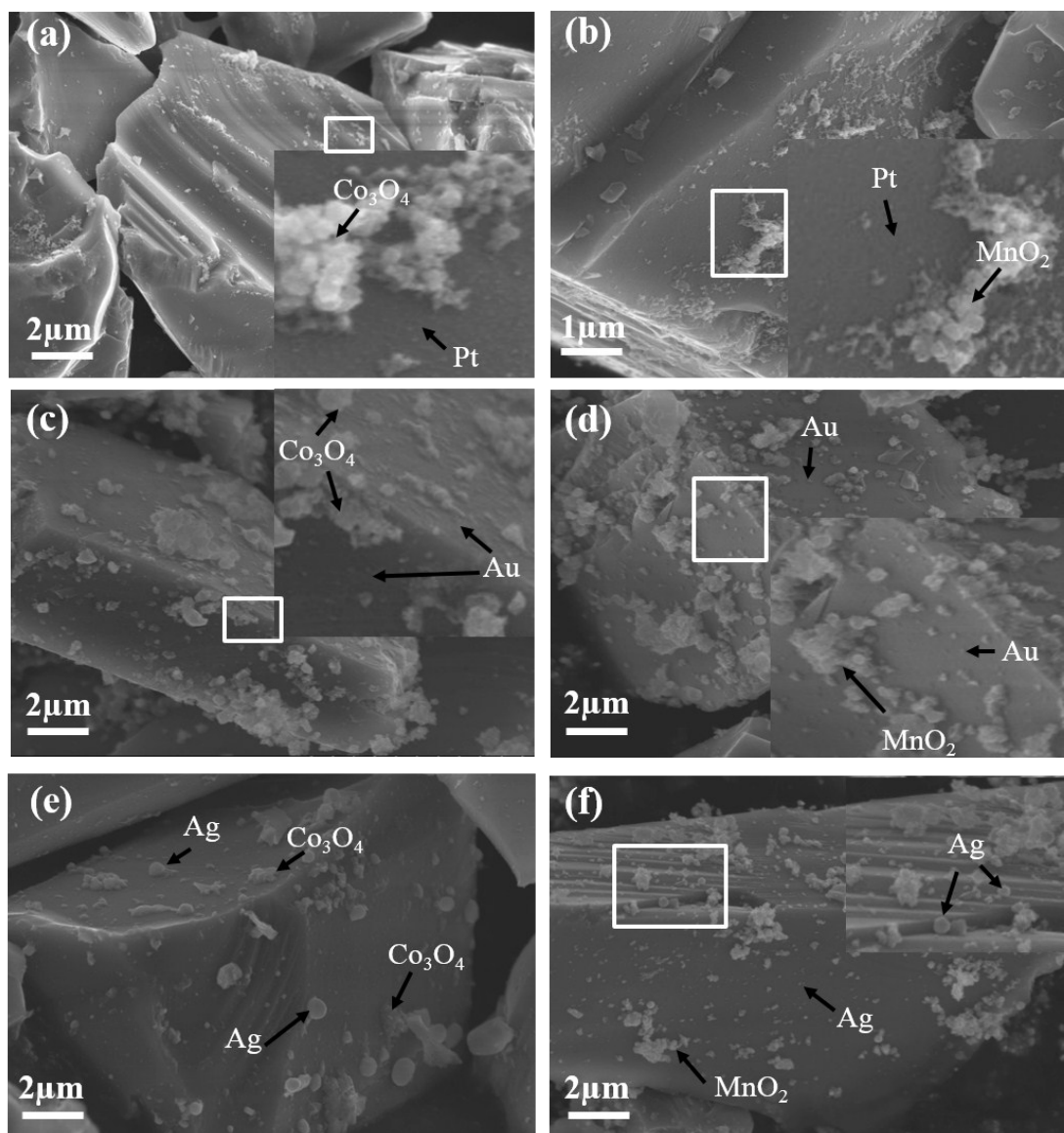


Fig. S8. The SEM images of dual cocatalysts deposited on SiC by impregnation method: (a) Pt/SiC/Co<sub>3</sub>O<sub>4</sub>, (b) Pt/SiC/MnO<sub>2</sub>, (c) Au/SiC/Co<sub>3</sub>O<sub>4</sub>, (d) Au/SiC/MnO<sub>2</sub>, (e) Ag/SiC/Co<sub>3</sub>O<sub>4</sub>, (f) Ag/SiC/MnO<sub>2</sub>. The light cluster is metal oxide (Co<sub>3</sub>O<sub>4</sub> or MnO<sub>2</sub>). The small dark granular is metal (Au and Pt). And the large circular nanoparticle is Ag.

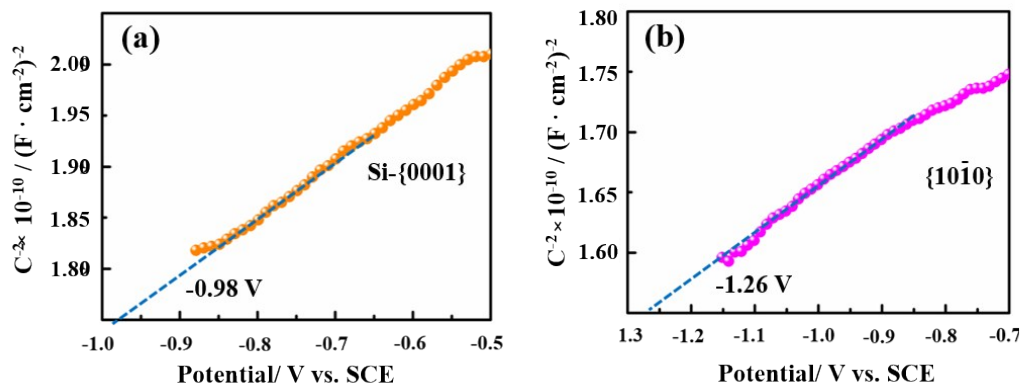


Fig. S9. The Mott-Schottky curves for the (a) Si-{0001} and (b) {10-10} facets were measured in  $\text{Na}_2\text{SO}_4$  solution.

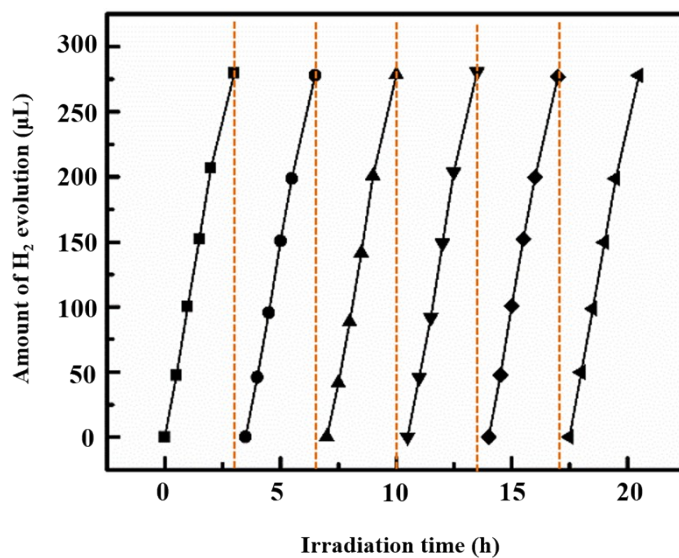


Fig. S10. Recycle test for  $\text{H}_2$  evolution over the samples Pt/SiC/ $\text{MnO}_2$  under visible light irradiation.

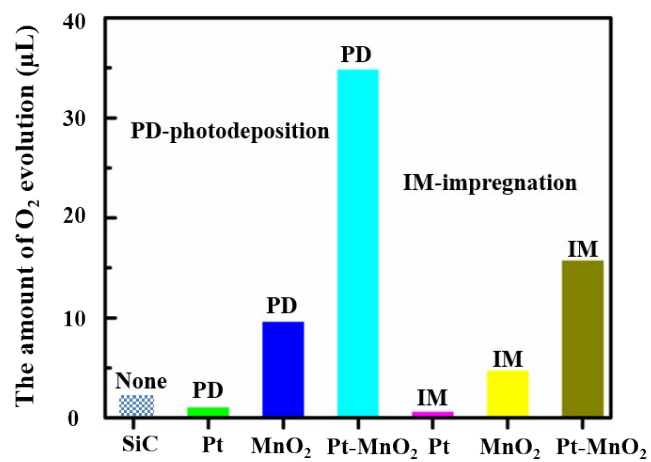


Fig. S11. Oxygen evolution over the samples by photodeposition and impregnated using AgNO<sub>3</sub> as sacrificial reagent.

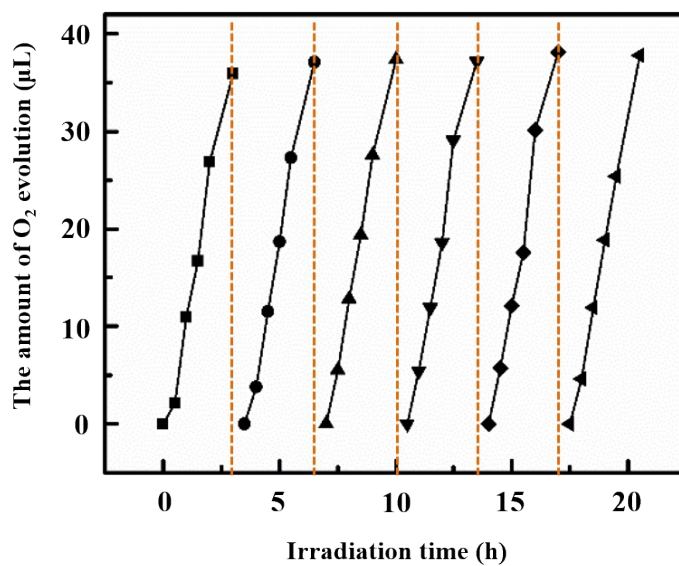


Fig. S12. Recycle test for O<sub>2</sub> evolution over the samples Pt/SiC/MnO<sub>2</sub> under visible light irradiation.

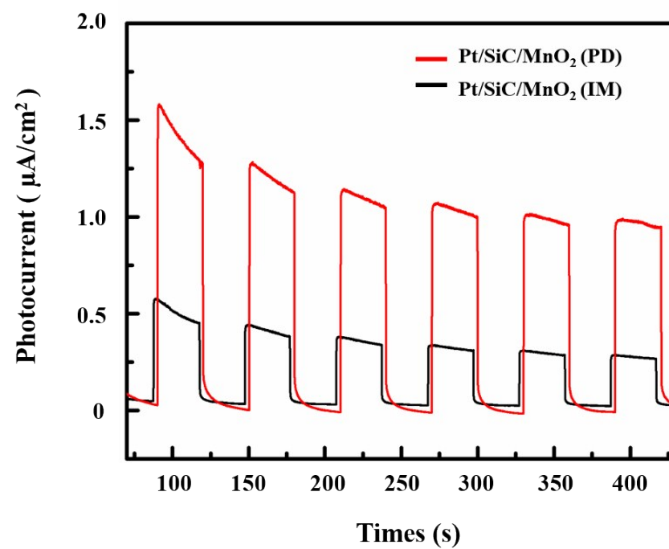


Fig. S13. Photocurrent (i-t curve) of Pt/SiC/MnO<sub>2</sub> (PD) and Pt/SiC/MnO<sub>2</sub> (IM). The downward trend at the first two irradiation process for both two samples is probably due to the unbalanced interfacial photocurrent.

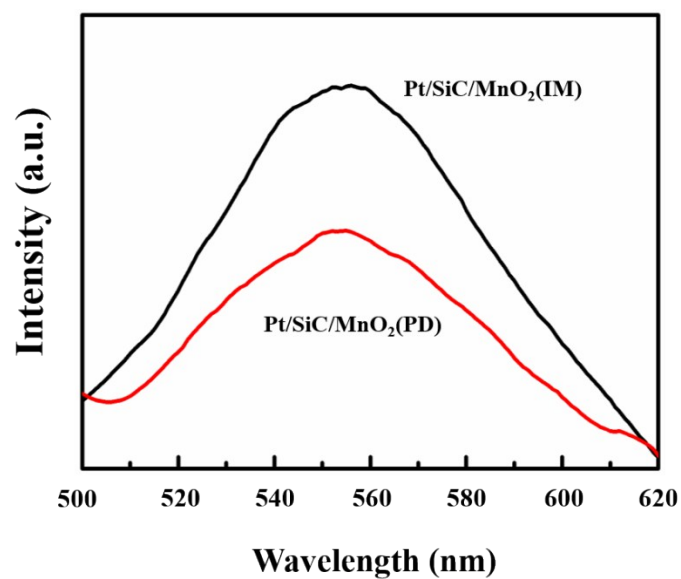


Fig. S14. Photoluminescence spectra of Pt/SiC/MnO<sub>2</sub> (PD) and Pt/SiC/MnO<sub>2</sub> (IM).

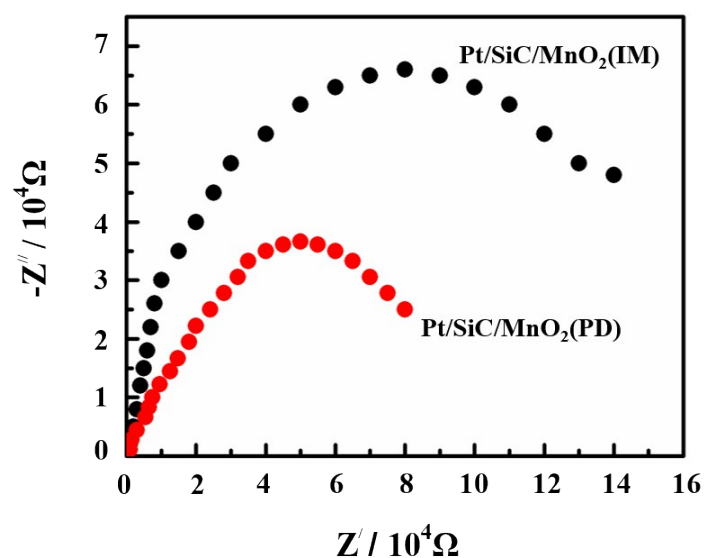


Fig. S15. Electrochemical impedance spectra of Pt/SiC/MnO<sub>2</sub> (PD) and Pt/SiC/MnO<sub>2</sub> (IM). The EIS Nyquist plots further reveal that the charges transfer rate is boosted by the selective deposition of cocatalysts, resulting in an effective separation of photo-generated electron-hole pairs.

Table S2 Photocatalytic water reduction activity of SiC with cocatalysts deposited by different methods.

Entry	Cocatalyst 1	Cocatalyst 2	H <sub>2</sub> Evolution rate (μmol·h <sup>-1</sup> ·g <sup>-1</sup> )
1	Pt (PD)	Co <sub>3</sub> O <sub>4</sub> (PD)	198
2	Pt (IM)	Co <sub>3</sub> O <sub>4</sub> (IM)	24.9
3	Co <sub>3</sub> O <sub>4</sub> (IM)	-	4.82
4	Co <sub>3</sub> O <sub>4</sub> (PD)	-	18.3

Note: PD means photodeposition, IM means impregnation.

Table S3 Photocatalytic water reduction activity of SiC with cocatalysts deposited by

photodeposition

Entry	Cocatalyst 1	Cocatalyst 2	H <sub>2</sub> Evolution rate ( $\mu\text{mol}\cdot\text{h}^{-1}\cdot\text{g}^{-1}$ )
1	Au	-	52.1
2	Au	MnO <sub>2</sub>	283
3	Au	Co <sub>3</sub> O <sub>4</sub>	221
4	Ag	-	38.2
5	Ag	MnO <sub>2</sub>	147
6	Ag	Co <sub>3</sub> O <sub>4</sub>	122

Table S4 Photocatalytic water reduction activity of SiC with cocatalysts deposited by impregnation

Entry	Cocatalyst 1	Cocatalyst 2	H <sub>2</sub> Evolution rate ( $\mu\text{mol}\cdot\text{h}^{-1}\cdot\text{g}^{-1}$ )
1	Au	-	11.5
2	Au	MnO <sub>2</sub>	40.1
3	Au	Co <sub>3</sub> O <sub>4</sub>	37.1
4	Ag	-	16.9
5	Ag	MnO <sub>2</sub>	50.4
6	Ag	Co <sub>3</sub> O <sub>4</sub>	35.3